

Article

Effect of Isotopic Substitution on Elementary Processes in Dye-Sensitized Solar Cells: Deuterated Amino-Phenyl Acid Dyes on TiO₂

Sergei Manzhos^{1,*}, Hiroshi Segawa^{2,†} and Koichi Yamashita^{3,†}

¹ Department of Mechanical Engineering, Faculty of Engineering, National University of Singapore, Blk EA, #07-08, 9 Engineering Drive 1, Singapore 117576, Singapore

² Research Center for Advanced Science and Technology (RCAST), The University of Tokyo, 4-6-1, Komaba, Meguro-ku, Tokyo 153-8904, Japan; E-Mail: csegawa@mail.ecc.u-tokyo.ac.jp

³ Department of Chemical System Engineering, School of Engineering, University of Tokyo, 7-3-1, Hongo, Bunkyo-ku, Tokyo 113-8656, Japan; E-Mail: yamasita@chemsys.t.u-tokyo.ac.jp

† These authors contributed equally to this work.

* Author to whom correspondence should be addressed; E-Mail: mpemanzh@nus.edu.sg; Tel.: +65-6516-4605; Fax: +65-6779-1459.

Received: 23 January 2013; in revised form: 4 February 2013 / Accepted: 1 March 2013 / Published: 11 March 2013

Abstract: We present the first computational study of the effects of isotopic substitution on the operation of dye-sensitized solar cells. *Ab initio* molecular dynamics is used to study the effect of deuteration on light absorption, dye adsorption dynamics, the averaged over vibrations driving force to injection (ΔG_i) and regeneration (ΔG_r), as well as on promotion of electron back-donation in dyes NK1 (2E,4E-2-cyano-5-(4-dimethylaminophenyl)penta-2,4-dienoic acid) and NK7 (2E,4E-2-cyano-5-(4-diphenylaminophenyl)penta-2,4-dienoic acid) adsorbed in monodentate molecular and bidentate bridging dissociative configurations on the anatase (101) surface of TiO₂. Deuteration causes a red shift of the absorption spectrum of the dye/TiO₂ complex by about 5% (dozens of nm), which can noticeably affect the overlap with the solar spectrum in real cells. The dynamics effect on the driving force to injection and recombination (the difference between the averaged $\langle \Delta G_{i,r} \rangle$ and $\Delta G_{i,r}^{\text{equil}}$ at the equilibrium configuration) is strong, yet there is surprisingly little isotopic effect: the average driving force to injection $\langle \Delta G_i \rangle$ and to regeneration $\langle \Delta G_r \rangle$ changes by only about 10 meV upon deuteration. The nuclear dynamics enhance recombination to the dye ground state due to the approach of the electron-donating group

to TiO₂, yet this effect is similar for deuterated and non-deuterated dyes. We conclude that the nuclear dynamics of the C-H(D) bonds, mostly affected by deuteration, might not be important for the operation of photoelectrochemical cells based on organic dyes. As the expectation value of the ground state energy is higher than its optimum geometry value (by up to 0.1 eV in the present case), nuclear motions will affect dye regeneration by recently proposed redox shuttle-dye combinations operating at low driving forces.

Keywords: dye-sensitized solar cells; molecular dynamics; deuteration; isotopic substitution; electron injection; recombination; dye regeneration

1. Introduction

Photoelectrochemical cells, such as dye-sensitized solar cells (DSSC) [1], have attracted considerable and renewed interest in recent years as a possible economic alternative to silicon cells, as some long-standing issues begin to be effectively resolved [2–5]. In a typical DSSC [1], a surface of a wide band gap (oxide) semiconductor anode (with a gap too wide to adsorb most visible light photons) is covered-sensitized by dye molecules. The dye absorbs the solar radiation and is thereby promoted to an excited state, whose energy lies within the conduction band (CB) of the oxide. The large density of states of the CB favors the electron transfer from the molecule to the oxide [6]. The electron can travel through the external circuit, and the resulting dye cation can be regenerated by a redox species in the electrolyte that provides ionic conductance between the sensitized surface and the cathode [7,8].

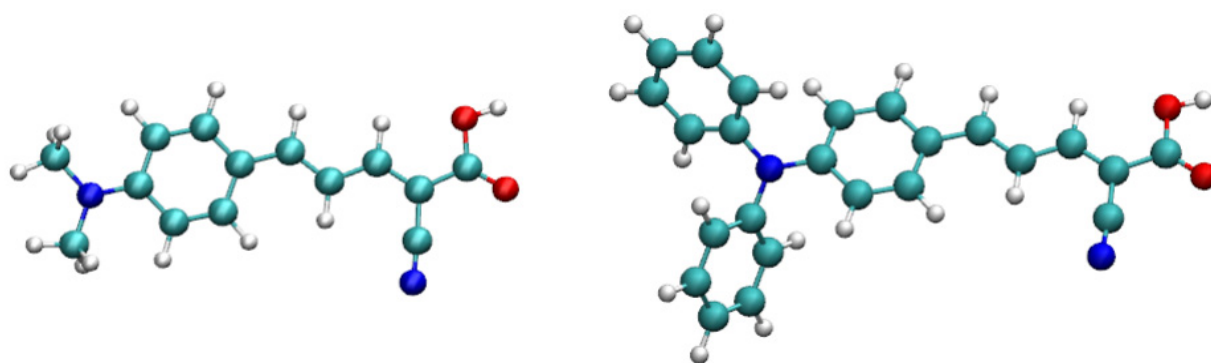
Besides the light absorption spectrum of the (adsorbed) chromophore molecule, the performance of photoelectrochemical cells largely depends on the kinetic competition between electron injection (charge separation) and dye regeneration (the desired processes), on one hand, and dye de-excitation and charge recombination of injected electrons with the dye cation or with electrolyte species, on the other (undesired processes) [1]. All these elementary processes are due to nuclear motions. Electron injection proceeds either via a non-adiabatic mechanism of transition between different electronic states—from one localized on the dye to one localized on the semiconductor—which is governed by derivative coupling, or via an adiabatic mechanism, with nuclei moving over a barrier on the potential energy surface [9,10]. The rates of dye de-excitation (internal conversion), regeneration, and electron recombination are also governed by the interaction of electronic and nuclear degrees of freedom [11–15]. A key parameter governing the rates of injection and regeneration is the driving force, which can be proxied as the difference between the energies of the molecular excited state and the conduction band minimum (CBM) for injection and between the redox potential of the redox species and the dye ground state, for regeneration.

Nuclear motions not only affect injection and recombination—they also result in a broadening and a shift of the light absorption spectrum [16,17]. This is because structural changes induce shifts in energy levels. These shifts can significantly modify rates of various electronic processes to the point of making predictions based solely on optimized geometries unreliable. For example, we have shown in [18] that nuclear dynamics can modify the driving force to injection by tenths of eV *vs.* the equilibrium geometry for organic dyes adsorbed on the anatase (101) surface of TiO₂, which could

result in an up to an order of magnitude change in the injection rate. The magnitude of this dynamic effect was also dependent on the dye adsorption configuration on TiO₂ (monodentate or bidentate). In [19], we predicted with molecular dynamics simulations that the rate of recombination of the injected electron with the dye cation can be enhanced by orders of magnitude by nuclear motions.

It is clear that nuclear dynamics is an important factor and that the ability to control it is a way to control the electron dynamics and, with it, the overall performance of photoelectrochemical solar cells. One way to modify nuclear dynamics is structural changes of the dye or dye-surface complex [20,21]. Such changes lead to a simultaneous modification of the electronic structure, and it could be difficult to optimize both. An example of a system where a structural change leading to a desirable electronic effect—increase in photon absorption and a better overlap with the solar spectrum—also leads to undesirable effects on electron-nuclear dynamics is the dyes *2E,4E*-2-cyano-5-(4-dimethylaminophenyl)penta-2,4-dienoic acid (referred to below as NK1) and *2E,4E*-2-cyano-5-(4-diphenylaminophenyl)penta-2,4-dienoic acid (referred to below as NK7), shown in Figure 1. NK7 differs from NK1 by an extended π -conjugation of the electron donor moiety—a typical procedure in organic dye design. The injection rate of the excited electrons from NK7 into titania was measured to be significantly lower compared to NK1 [22]. Likely reasons for this are increased electron-phonon coupling [12] and a less favorable energy level matching with TiO₂ [18].

Figure 1. *2E,4E*-2-cyano-5-(4-dimethylaminophenyl)penta-2,4-dienoic acid (NK1) (left) and *2E,4E*-2-cyano-5-(4-diphenylaminophenyl)penta-2,4-dienoic acid (NK7) (right) dyes. Atom colors here and elsewhere: *N*–blue, *C*–turquoise, *O*–red, *H*–grey and Ti–black.



It is, therefore, important to explore possibilities of modifying nuclear dynamics without seriously affecting equilibrium electronic structure. This is in principle possible by: (i) introducing steric hindrance, for example, by using co-adsorbates; (ii) controlling the temperature; and (iii) isotopic substitution. The use of co-adsorbates is widespread, due to their ability to shift the conduction band minimum (CBM) of the oxide and to prevent recombination [23–26]. We have recently observed in molecular dynamics simulations that co-adsorbed water can prevent a close approach of the dye-equivalent oxidation hole to TiO₂, which should hinder recombination with the dye cation [17,19]. Most co-adsorbates used in DSSC do, however, modify the electronic structure of the oxide surface [17,24–26]. In the Born-Oppenheimer approximation, temperature can change the vibrational dynamics of low-frequency modes without affecting electronic structure. A recent theoretical study of the temperature effect in the range 300–350 K on absorption, injection, and recombination in DSSC

predicted that an increase in temperature would cause a red-shift in the absorption spectrum, but little effect on the driving force to injection, while definitive conclusions about the effect on recombination could not be drawn, due to a small time-frame of the simulations (10 ps) [19]. While other systems could potentially be identified with stronger temperature dependence, it would likely be impractical to thermostat a real solar cell in order to maintain the optimal temperature.

Isotopic substitution, on the other hand, appears to be a much cleaner way to impact nuclear dynamics without affecting electronic structure and without changing the dye structure or environment. It will change the amplitude of atomic vibrations, as well as directions of normal mode vectors. This will affect the (averaged over nuclear vibrations) molecular energy levels [18], as well as the values of derivative coupling elements responsible for nonadiabatic transitions [13,15,27]. Isotopic substitution has been used to increase the excited state lifetime of organic molecules and transition metal complexes used in organic light-emitting diodes (OLED), in order to increase the luminescence yield by reducing the rate of nonradiative decay, due to vibronic coupling [28–31], but studies of the isotopic effect on the performance of photoelectrochemical cells are almost non-existent. We have recently estimated the effect of deuteration of tetracyanoethylene (TCNE), tetracyanoquinodimethane (TCNQ) and tetracyanoanthraquinodimethane (TCNAQ) on the geminate recombination in cells utilizing interfacial charge transfer bands (so-called direct injection cells) [13]. It was predicted that deuteration significantly changes the contribution of many vibrational modes to the rate of geminate recombination, although the overall effect was mild, as the main promoting modes were little affected. To the best of our knowledge, no study of the effects of isotopic substitution on the performance of the conventional DSSC's has been done.

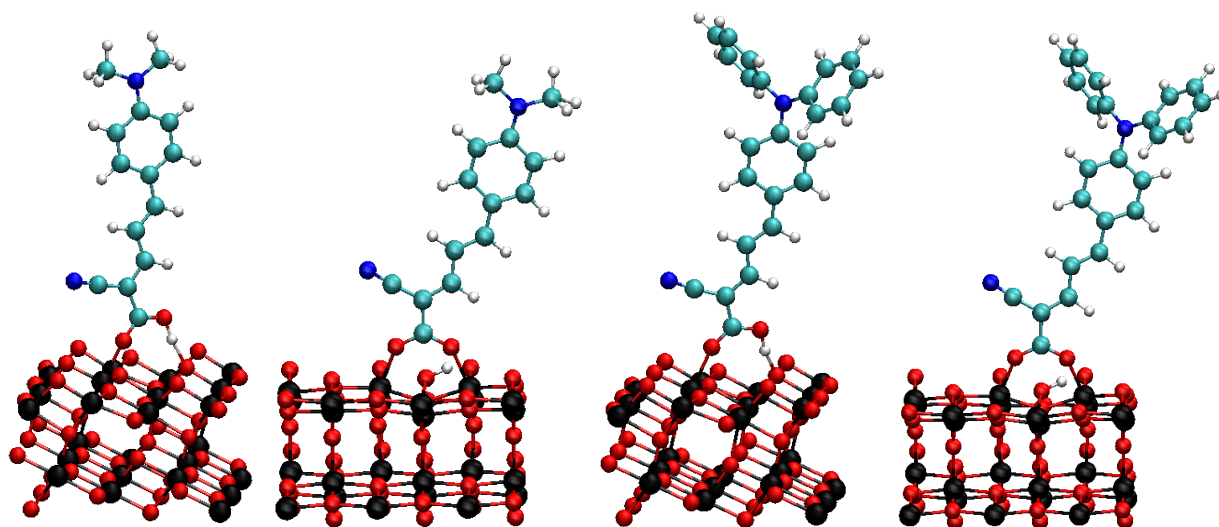
Here, we study how deuteration—the most readily achievable type of isotopic substitution [31–33]—can change the nuclear dynamics effect on light absorption, electron injection, and recombination in NK1 and NK7 dyes on TiO_2 . The paper is organized as follows: in Section 2, theoretical and computational methods are described, Section 3 presents the results of comparative studies of the dynamical effects in deuterated and non-deuterated dyes, and Section 4 concludes.

2. Theoretical and Computational Methods

The methodology here is similar to that used in [18,19], namely, the electronic and molecular structure was computed using DFT (density functional theory) [34] and the SIESTA code [35]. The Perdew-Burke-Ernzerhof (PBE) exchange-correlation functional [36] and the DZP basis set (double- ζ polarized orbitals) were used. We used a standard DZP basis set as generated by SIESTA, but the cutoff radii were increased from the default values by choosing $E_{\text{shift}} = 0.001$ Ry to mitigate basis-set superposition errors [37]. A large enough simulation cell was used that the Brillouin zone was sampled at the Γ point ($11.36 \times 10.25 \times 27.0/30.0$ Å for the cells containing NK1/NK7 dyes, respectively). Core electrons are treated within the effective core approximation with Troullier-Martins pseudopotentials (provided with SIESTA) [38]. Geometries were optimized until forces on non-fixed atoms were below 0.02 eV/Å. The TiO_2 anatase (101) surface was used, as it is the dominant and thermodynamically stable facet [39]. It was modeled with a 3×1 slab containing four Ti layers, of which two top Ti layers were allowed to move and the bottom layers were kept frozen at their bulk position. DFT values for TiO_2 lattice constants of $a, c = 3.78, 9.52$ Å are in excellent agreement with

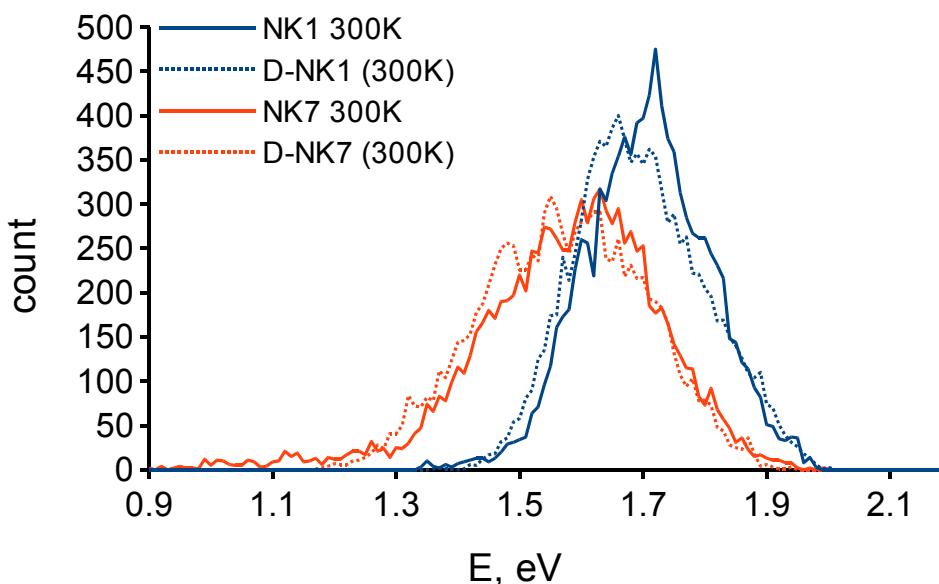
the experiment and other theoretical calculations [40]. This slab thickness was shown to be adequate to simulate dye adsorption and electron injection [41–44]. *Ab initio* molecular dynamics (MD) simulations were performed at 300 K using a Nose-Hoover thermostat with a time step of 1 fs. The first 3 ps were discarded for equilibration before computing distributions and averages (for which data were sampled every time step). These parameters are similar to other dynamical studies of dye/titania systems [45,18,46]. The MD trajectories for free dyes were 10 ps long, which was sufficient to sample all intermolecular vibrations. In [19], we identified that the MD trajectory needs to be longer than 10 ps in order to account for orientational degrees of freedom of the dye with respect to the surface. Here, we therefore computed 15 ps-long trajectories for deuterated (referred to below as D-NK1 and D-NK7) and non-deuterated NK1 and NK7 dyes adsorbed on a clean surface in the monodentate and bidentate bridging configurations, for a total of eight MD simulations. As a result, the post-equilibration parts of the trajectories used to estimate the averages are almost twice as long compared to [18,19]. Figure 2 shows the optimized geometries, which served as the starting point for the MD calculations. Full deuteration is assumed.

Figure 2. Optimized monodentate (left in each pair) and bidentate (right in each pair) adsorption configurations of dyes NK1 (**left pair**) and NK7 (**right pair**) on the anatase (101) surface of TiO₂.



The effect of nuclear motions of deuterated and non-deuterated dyes on the absorption spectra was estimated from the distributions obtained during MD of the HOMO-LUMO gap for free dyes or HOMO-LUMO* for adsorbed dyes, where LUMO* are orbitals of the adsorbate complex corresponding to the dye LUMO (average energies are used when there is more than one LUMO*; see [18] for more details). We have shown previously that the gap reproduces well the relative spectra in spite of the underestimation of the absolute energies when using a generalized gradient approximations (GGA) functional [16]. The effect on the driving force to injection was estimated by comparing $\Delta G_i = \text{LUMO}^* - \text{CBM}$, at the equilibrium, $\Delta G_i^{\text{equil}}$, and averaged over MD trajectories, $\langle \Delta G_i \rangle$. As isotopic substitution does not affect the equilibrium geometry and electronic structure, the initial configurations and their frontier orbitals are the same as in the previous study (see Figures 1–3 of [18]).

Figure 3. Distributions of the HOMO-LUMO gap for free NK1 (blue) and NK7 (red) dyes during MD. Solid lines are for non-deuterated and dotted lines are for deuterated molecules.



3. Results and Discussion

3.1. Effect of Deuteration on Absorption Spectra and Dye Regeneration

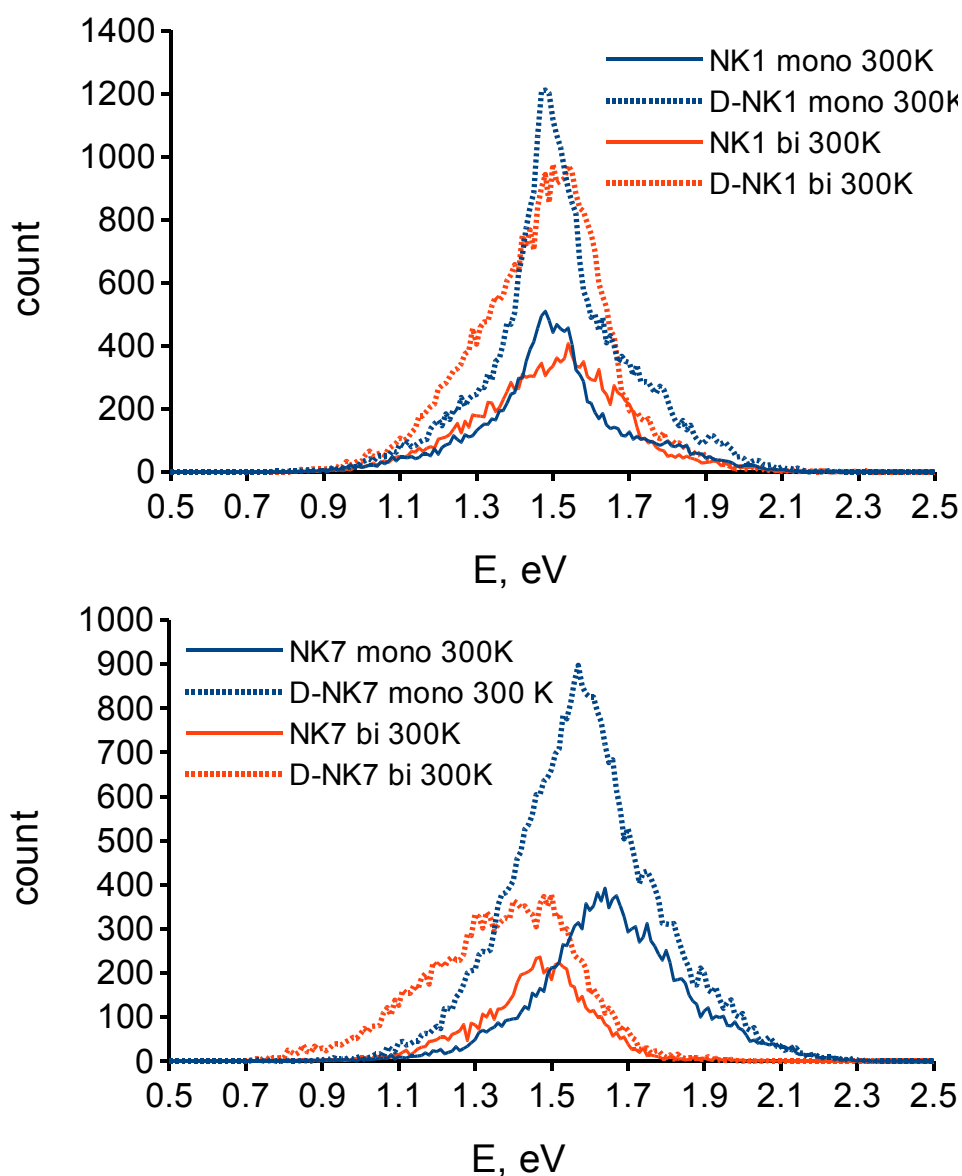
The distributions of the highest occupied molecular orbital and lowest unoccupied molecular orbital (HOMO-LUMO) gap of the free dyes during the MD trajectories are shown in Figure 3. Nuclear vibrations cause not only a broadening of the electronic transitions, but also a red shift. The expectation value of the gap for NK1 is 1.70 eV vs. 1.88 eV at the equilibrium geometry. The corresponding values for NK7 are 1.57 eV and 1.70 eV. The lowering of the gaps is due to a destabilization of the HOMO (from -5.37 to -5.27 eV for NK1, from -5.52 to -5.36 for NK7) rather than to a stabilization of the LUMO (from -3.49 to -3.57 for NK1, a slight increase from -3.82 to -3.79 for NK7), on the average, during vibrations.

In a classic MD simulation (where the nuclei are treated classically and move on the Born-Oppenheimer potential energy surface computed quantum mechanically), deuteration is not expected to change this pattern, and indeed, the nuclear motions cause a similar red shift, with the expectation values of the gap of 1.69 and 1.56 eV for D-NK1 and D-NK7, respectively. The difference in the spectral shape can be appreciated visually by comparing solid and dotted lines in Figure 3. Overall, the computed effect of deuteration on light absorption of the free dyes is negligible and is within numeric accuracy.

For dyes adsorbed on TiO_2 , the comparison of spectral shapes between NK1 and NK7 and D-NK1 and D-NK7 is given in Figure 4. There is a noticeable dynamical effect on the spectrum in that the expectation value of the HOMO-LUMO* gap is 1.48/1.52 eV and 1.66/1.59 compared to the equilibrium values of 1.70 and 1.59 eV for NK1/D-NK1 and NK7/D-NK7, respectively, in the case of monodentate adsorption. For the bidentate adsorption, the expectation value of the HOMO-LUMO* gap is 1.47/1.48 eV and 1.45/1.39 compared to the equilibrium values of 1.70 and 1.53 eV for

NK1/D-NK1 and NK7/D-NK7, respectively. Dynamical lowering of the gap is due to a destabilization of the HOMO (similarly to the case of the free dyes), as well as a stabilization of the LUMO*, both by up to 0.1 eV (Table 1). The exception is NK7 adsorbed in the monodentate regime, where there is little difference in $\langle \text{HOMO} \rangle$ and $\langle \text{LUMO}^* \rangle$ vs. the equilibrium values for both deuterated and non-deuterated dye. This will be explained below by the specifics of dye motion with respect to the oxide surface in this system (Section 3.3).

Figure 4. Distributions of the highest occupied molecular orbital and lowest unoccupied molecular orbital (HOMO-LUMO*) gap for NK1 (**top**) and NK7 (**bottom**) dyes, adsorbed on the anatase (101) surface of TiO₂ in the monodentate (blue) and bidentate (red) regimes during molecular dynamics (MD). Solid lines are for non-deuterated and dotted lines are for deuterated molecules. Arbitrary units. (The areas under the curves for the mono- and bi-dentate configurations are not always equal, because different numbers of orbitals have the character of the dye's LUMO [18]. Curves for the deuterated dyes are magnified for better visibility).



While deuteration has little effect on the HOMO-LUMO* gap in NK1/TiO₂, there is clearly a red shift induced by isotopic substitution in D-NK7/TiO₂. Such a dependence on molecular structure can be rationalized by the presence of floppy C₆H₅ moieties in NK7. The low-frequency torsional dynamics of these moieties can be impacted to a larger degree by deuteration than the CH₃ ligands in NK1 and, with it, the overall vibrational dynamics of the molecular backbone. The resulting larger deviations from the equilibrium geometry are likely to enhance the dynamical effect on the spectrum, *i.e.*, the red shift. Why did this effect appear in the adsorbed, but not in the free dyes? The answer must lie in the orientational motions with respect to the surface of TiO₂. There is a significant hybridization of molecular energy levels with those of the oxide [18], and these motions are expected to influence the energies of the adsorbate complex, while molecular orientation has no effect on energy levels of a free dye. Indeed, in D-NK7/TiO₂, the expectation values of HOMO are increased and simultaneously the expectation values of LUMO* are lowered by up to 0.04 eV each *vs.* H-NK7/TiO₂. As a result, the spectrum is red-shifted by about 0.1 eV or about 5%–6%. Considering typical underestimation of the gap by GGA DFT, this should result in a shift on the order of dozens of nm in real cells, which could have a significant effect on the overlap with the solar spectrum.

Table 1. The energies of the dyes' frontier orbitals and the gap between them, the energy of the conduction band minimum (CBM) of TiO₂ and the driving force to injection ΔG_i , in eV, at the equilibrium configuration and averaged over nuclear motions for the non-deuterated and deuterated NK1 and NK7 dyes adsorbed on TiO₂ in the monodentate and bidentate configurations, as shown in Figure 2.

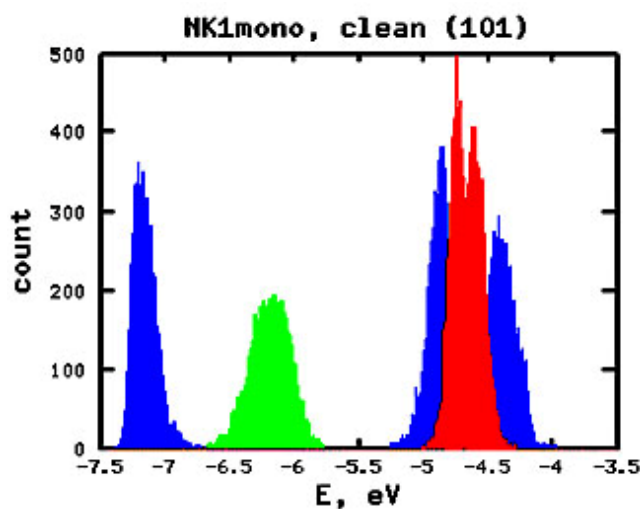
System	Equilibrium/MD averaged (non-deuterated)/MD averaged (deuterated)				
	HOMO	LUMO*	gap	CBM	ΔG_i
NK1 mono	-6.26/-6.16/-6.18	-4.56/-4.67/-4.67	1.70/1.48/1.52	-4.69/-4.89/-4.88	0.13/0.23/0.22
NK1 bi	-6.11/-6.03/-6.06	-4.41/-4.56/-4.58	1.70/1.47/1.48	-4.84/-4.98/-5.00	0.43/0.42/0.42
NK7 mono	-6.19/-6.23/-6.19	-4.60/-4.58/-4.61	1.59/1.66/1.59	-4.72/-4.79/-4.82	0.11/0.21/0.22
NK7 bi	-6.10/-6.04/-6.02	-4.57/-4.59/-4.63	1.53/1.45/1.39	-4.84/-4.92/-4.94	0.28/0.32/0.31

The average over nuclear motions energy of the dye ground state permits a preview into the effect of nuclear motions on regeneration. As room temperature vibrations are able to destabilize the HOMO level in (deuterated or non-deuterated) dyes/TiO₂, this could decrease the driving force to regeneration $\langle \Delta G_r \rangle$ by the electrolyte by up to 0.1 eV *vs.* the static estimate $\Delta G_r^{\text{equil}}$, which could have a noticeable effect on the regeneration rate, depending on the redox shuttle used [7,8]. This effect is expected to be important for the development of new redox shuttles, which operate at low driving forces, to gain a higher open-circuit voltage—which is currently an area of active research [7,8]. Indeed, it has been established that effective regeneration can be possible with ΔG_r as low as 0.2–0.3 eV, and a number of redox shuttle-dye couples operating in these regimes have been proposed [7,8,47–49]. On the other hand, the deuteration effect on the regeneration rate is unlikely to be significant, as the change in the average HOMO level predicted here is within 0.05 eV.

3.2. Effect of Deuteration on Injection Conditions

Even as the equilibrium electronic structure is the same for H-NK1,7 and D-NK1,7, deuteration is expected to influence injection conditions via different nuclear dynamics, as normal mode vectors are mass-dependent. This affects the temporal distribution of the adsorbate system's energy levels and its average over nuclear motions. In Table 1, we list the driving force to injection in the eight systems: at the equilibrium geometry $\Delta G_i^{\text{equil}}$ and averaged over nuclear motions $\langle \Delta G_i \rangle$, for the non-deuterated and deuterated dyes. An example distribution of the energy levels relevant for electron injection and dye regeneration following from the MD trajectory of the dye/TiO₂ system is shown in Figure 5. The distributions are similar to those reported in [18] for shorter (10 ps) trajectories and for non-deuterated dyes and do not visually differ between deuterated and non-deuterated dyes. These calculations showed that nuclear motions exert a strong effect on injection conditions, with the expectation values of ΔG_i differing by up to 0.1 eV from those computed at the equilibrium geometry. This dynamic effect is dependent on the dye molecular structure, as well as on the adsorption mode, being stronger for monodentate adsorption. The magnitude of the difference between $\langle \Delta G_i \rangle$ and $\Delta G_i^{\text{equil}}$ is significant, as it has been estimated that the injection rate changes by a factor of two when ΔG_i changes by 100 meV [50,51].

Figure 5. Distributions following from an MD trajectory of energy levels relevant for light absorption, electron injection and dye regeneration for the NK1 dye adsorbed on TiO₂ in the monodentate configuration (see Figure 2). Blue: TiO₂ valence band maximum (VBM) and conduction band (CB) levels, green–HOMO, red–LUMO*.



It is striking that despite the fact that the dynamic effect (the difference between $\Delta G_i^{\text{equil}}$ and $\langle \Delta G_i \rangle$) is large, deuteration has a negligible effect on $\langle \Delta G_i \rangle$. This must mean that it is the distribution of configurations of the molecular backbone that determines the dynamic effect on injection and that the nuclear dynamics of the CH(CD) bonds do not affect this distribution much. Interestingly, it was recently shown that deuteration does not change the rates of geminate recombination much in organic dye/TiO₂ adsorbate complexes, which are also driven by the nuclear dynamics [13]. This suggests that deuteration may not be an effective way to control electronic processes which depend on the

backbone's structure and dynamics. The question remains open whether other types of isotopic substitution (in the backbone itself) could achieve such control.

3.3. Effect of Deuteration on Orientational Motions and Recombination to the Dye Cation

In Figure 6, we show the temporal evolution of the distance, z , between the amino group and the oxide surface for all studied cases. It shows an approach of the electron donating group to the surface, which is a purely dynamic effect and is not due to a lower electronic energy in the tilted configuration, as discussed in [19]. It will have an enormous effect on the back-donation rate, which has been shown to depend exponentially on this distance [52,53]:

$$\tau_{rec}^{-1} = Ae^{-\beta z} \quad (1)$$

Here, we observe that deuteration does little to change it, even if the details of the dynamics are different. This can be rationalized, on one hand, by a relatively small change of the dye molecular mass due to deuteration, which is not expected to have a strong effect on how the configuration space of orientational degrees of freedom is sampled, and, on the other hand, by the fact that the amplitude of vibrations, including dye wagging around the surface, is mass-independent in classical MD.

Figure 6. Temporal evolution of the distance between the amino group's N atom and the TiO₂ surface for NK1 (**top**) and NK7 (**bottom**) dyes, adsorbed in the monodentate (blue) and bidentate (red) regimes during MD. Solid lines are for non-deuterated (H-), and dotted lines are for deuterated (D-) molecules.

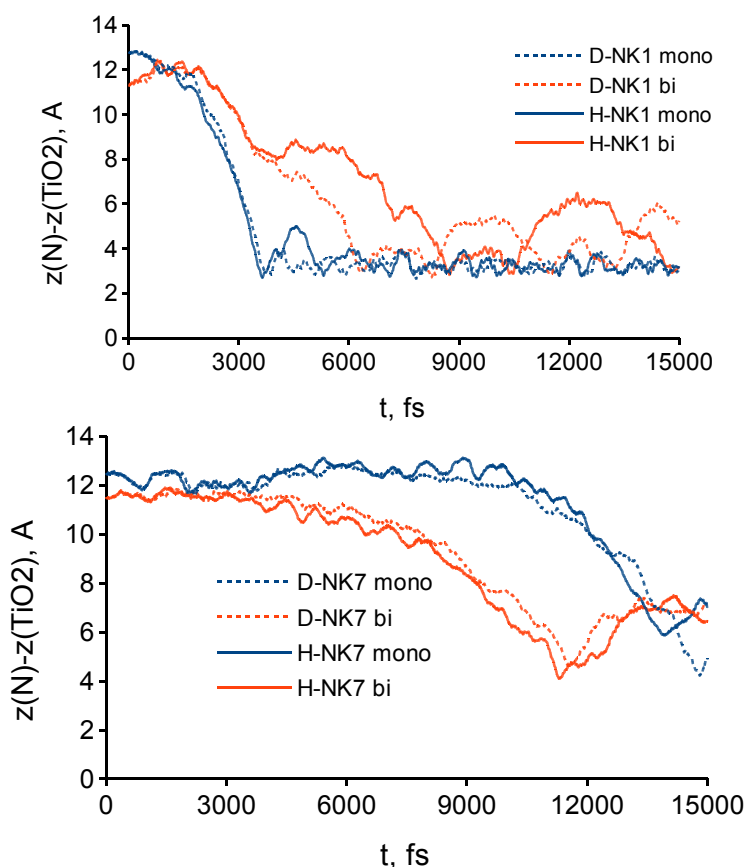


Figure 6 also shows that the (H-, D-) NK7 dye adsorbed in the monodentate configuration spends most of the trajectory in a near vertical configuration (Figure 2), with a significant tilt occurring only after 10 ps. This explains the smaller destabilization of the frontier orbitals by nuclear motions *vs.* the other systems described in Section 3.1 and corroborates the idea that orientational motions with respect to the surface play an important role in the dynamical effect on energy levels and in the red-shift of the absorption spectrum predicted in Section 3.1.

4. Conclusions

We have studied the effect of an isotopic substitution—deuteration—on the conditions determining the efficiency of dye-sensitized solar cells, namely, light absorption and energy level matching, which, in turn, determines the rates of electron injection and recombination and of dye regeneration by electrolyte species. Nuclear dynamics affect the electronic structure and energy levels of the dye-semiconductor system by modulating its molecular structure. This nuclear dynamics effect can be significant, and here, we investigated how it can be modulated by using isotopic substitution. In a classical MD study, it is impossible to capture the quantum isotopic effects, such as changes in the zero-point energy, which will also affect the average geometry. The classical study presented here captures the isotopic effect wrought via changes in the direction and amplitude of atomic vibrations. This mass-dependence is unique to polyatomic molecules in a non-isotropic space (the presence of the surface) when masses of all atoms do not change in the same proportion, as reflected in the mass-dependence of normal mode displacement vectors, in contrast to a one-dimensional classical oscillator, where the amplitude of vibrations and the average geometry are mass-independent at a given total energy. While the thermostat imposes the same average kinetic and, therefore, potential energy, in a multi-atomic system, these can be realized at different average conformations.

We found a noticeable effect of deuteration on the HOMO-LUMO gap of the adsorbate system, causing a red shift on the order of 5%, which should translate into a shift of dozens of nm in real cells and significantly impact the overlap of the absorption and the solar spectra. On the other hand, and surprisingly, the effect on energy level matching with the TiO₂ conduction band was negligible, *i.e.*, the difference between $\langle \Delta G_i^H \rangle$ and $\langle \Delta G_i^D \rangle$ is much smaller than between $\langle \Delta G_i^H \rangle$ and $\Delta G_i^{\text{equil}}$. This leads us to conclude that deuteration could be used to fine-tune vibrationally-averaged energy levels of adsorbed dyes, but not in a major way. This conclusion might not, however, hold for other isotopic substitutions.

Nuclear dynamics is likely to have a strong effect on the rate of parasitic electron back-donation from TiO₂ into the oxidation equivalent hole formed on the dye's electron-donating group upon injection. The approach of this group to the oxide surface can lead to an increase of the back-donation rate by orders of magnitude. Here, too, the effect of deuteration was found to be minor. Other strategies are therefore recommended to prevent a close approach to the surface of the electron donating group, such as the use of co-adsorbents [18].

Nuclear motions are likely to affect dye regeneration by the electrolyte, as the expectation value of the ground state energy can be higher *vs.* the static (optimum geometry) estimate, by about 0.1 eV in the present case. The development of efficient and mass-producible dye-sensitized cell is closely dependent on the development of alternative (to iodide/triiodide) redox shuttles, specifically those

which are able to operate at smaller driving forces to achieve a higher open-circuit voltage [7,8]. Redox species-dye combinations (e.g., Co-based [8,47,49] or ferrocene [48] redox shuttles combined with Ru-free dyes) operating at ΔG_r as low as 0.2–0.3 eV are being actively researched [7,8]. For such systems, the dynamic effect described here should be taken into account.

Acknowledgments

This work was supported by the Tier 1 AcRF grant from the Ministry of Education of Singapore.

Conflict of Interest

The authors declare no conflict of interest.

References

1. Hagfeldt, A.; Boschloo, G.; Sun, L.; Kloo, L.; Pattersson, H. Dye-sensitized solar cells. *Chem. Rev.* **2010**, *110*, 6595–6663.
2. Mora-Sero, I.; Bisquert, J. Breakthroughs in the development of semiconductor-sensitized solar cells. *J. Phys. Chem. Lett.* **2010**, *1*, 3046–3052.
3. Peter, L.M. The Grätzel cell: Where next? *J. Phys. Chem. Lett.* **2011**, *2*, 1861–1867.
4. Yella, A.; Lee, H.-W.; Tsao, H.N.; Yi, C.; Chandiran, A.K.; Nazeeruddin, M.K.; Diau, E.W.-G.; Yeh, C.-Y.; Zakeeruddin, S.M.; Grätzel, M. Porphyrin-sensitized solar cells with cobalt (II/III)-based redox electrolyte exceed 12 percent efficiency. *Science* **2011**, *334*, 629–634.
5. Yum, J.-H.; Baranoff, E.; Kessler, F.; Moehl, T.; Ahmad, S.; Bessho, T.; Marchioro, A.; Ghadiri, E.; Moser, J.-E.; Yi, C.; Nazeeruddin, Md.K.; Grätzel, M. A cobalt complex redox shuttle for dye-sensitized solar cells with high open-circuit potentials. *Nat. Commun.* **2012**, *3*, 631:1–631:8.
6. Martsinovich, N.; Troisi, A. Theoretical studies of dye-sensitized solar cells: From electronic structure to elementary processes. *Energy Environ. Sci.* **2011**, *4*, 4473–4495.
7. Cong, J.; Yang, X.; Kloo, L.; Sun, L. Iodine/iodide-free redox shuttles for liquid electrolyte-based dye-sensitized solar cells. *Energy Environ. Sci.* **2012**, *5*, 9180–9194.
8. Wang, M.; Grätzel, C.; Zakeeruddin, S.M.; Grätzel, M. Recent developments in redox electrolytes for dye-sensitized solar cells. *Energy Environ. Sci.* **2012**, *5*, 9394–9405.
9. Prezhdo, O.V.; Duncan, W.R.; Prezhdo, V.V. Photoinduced electron dynamics at semiconductor interfaces: A time-domain ab initio prospective. *Progr. Surf. Sci.* **2009**, *84*, 30–68.
10. Duncan, W.R.; Prezhdo, O.V. Theoretical studies of photoinduced electron transfer in dye-sensitized TiO₂. *Annu. Rev. Phys. Chem.* **2008**, *58*, 143–184.
11. Manzhos, S.; Segawa, H.; Yamashita, K. A model for recombination in Type II dye-sensitized solar cells: Catechol-thiophene dyes. *Chem. Phys. Lett.* **2011**, *504*, 230–235.
12. Manzhos, S.; Segawa, H.; Yamashita, K. Derivative coupling constants of NK1, NK7 dyes and their relation to excited state dynamics in solar cell applications. *Chem. Phys. Lett.* **2011**, *501*, 580–586.

13. Manzhos, S.; Fujisawa, J.; Segawa, H.; Yamashita, K. Isotopic substitution as a strategy to control non-adiabatic dynamics in photoelectrochemical cells: Surface complexes between TiO₂ and dicyanomethylene compounds. *Jpn. J. Appl. Phys.* **2012**, *51*, 10NE03:1–10NE03:6.
14. Manzhos, S.; Jono, R.; Yamashita, K.; Fujisawa, J.; Nagata, M.; Segawa, H. A study of interfacial charge transfer bands and electron recombination in the surface complexes of TCNE, TCNQ, and TCNAQ with TiO₂. *J. Phys. Chem. C* **2011**, *115*, 21487–21493.
15. Niu, Y.; Peng, Q.; Deng, C.; Gao, X.; Shuai, Z. Theory of excited state decays and optical spectra: Application to polyatomic molecules. *J. Phys. Chem. A* **2010**, *114*, 7817–7831.
16. Manzhos, S.; Segawa, H.; Yamashita, K. Computational dye design by changing the conjugation order: Failure of LR-TDDFT to predict relative excitation energies in organic dyes differing by the position of the methine unit. *Chem. Phys. Lett.* **2012**, *527*, 51–56.
17. Manzhos, S.; Segawa, H.; Yamashita, K. Effect of nuclear vibrations, temperature, co-adsorbed water, and dye orientation on light absorption, charge injection and recombination conditions in organic dyes on TiO₂. *Phys. Chem. Chem. Phys.* **2013**, *15*, 1141–1147.
18. Manzhos, S.; Segawa, H.; Yamashita, K. The effect of ligand substitution and water co-adsorption on the adsorption dynamics and energy level matching of amino-phenyl acid dyes on TiO₂. *Phys. Chem. Chem. Phys.* **2012**, *14*, 1749–1755.
19. Manzhos, S.; Segawa, H.; Yamashita, K. Effect of nuclear vibrations, temperature, and orientation on injection and recombination conditions in amino-phenyl acid dyes on TiO₂. *Proc. SPIE* **2012**, *8438*, 843814:1–843814:10.
20. Lim, K.; Kim, C.; Song, J.; Yu, T.; Lim, W.; Song, K.; Wang, P.; Zu, N.; Ko, J. Enhancing the performance of organic dye-sensitized solar cells via a slight structure modification. *J. Phys. Chem. C* **2011**, *115*, 22640–22646.
21. Zhang, M.-D.; Pan, H.; Ju, X.-H.; Ji, Y.-J.; Qin, L.; Zheng, H.-G.; Zhou, X.-F. Improvement of dye-sensitized solar cells' performance through introducing suitable heterocyclic groups to triarylamine dyes. *Phys. Chem. Chem. Phys.* **2012**, *14*, 2809–2815.
22. Myllyperkio, P.; Manzoni, C.; Polli, D.; Cerullo, G.; Korppi-Tommola, J. Electron transfer from organic aminophenyl acid sensitizers to titanium dioxide nanoparticle films. *J. Phys. Chem. C* **2009**, *113*, 13985–13992.
23. Han, L.; Islam, A.; Chen, H.; Malapaka, C.; Chiranjeevi, B.; Zhang, S.; Yang, X.; Yanagida, M. High-efficiency dye-sensitized solar cell with a novel co-adsorbent. *Energy Environ. Sci.* **2012**, *5*, 6057–6060.
24. Long, H.; Zhou, D.; Zhang, M.; Peng, C.; Uchida, S.; Wang, P. Probing dye-correlated interplay of energetics and kinetics in mesoscopic titania solar cells with 4-tert-butylpyridine. *J. Phys. Chem. C* **2011**, *115*, 14408–14414.
25. Ren, X.; Feng, Q.; Zhou, G.; Huang, C.-H.; Wang, Z.-S. Effect of cations in coadsorbate on charge recombination and conduction band edge movement in dye-sensitized solar cells. *J. Phys. Chem. C* **2010**, *114*, 7190–7195.
26. Asuduzzaman, A.M.; Schreckenbach, G. Computational studies on the interactions among redox couples, additives and TiO₂: Implications for dye-sensitized solar cells. *Phys. Chem. Chem. Phys.* **2010**, *12*, 14609–14618.

27. Shizu, K.; Sato, T.; Tanaka, K. Vibronic coupling density analysis for α -oligothiophene cations: A new insight for polaronic defects. *Chem. Phys.* **2010**, *369*, 108–121.
28. Abe, T.; Miyazawa, A.; Konno, H.; Kawanishi, Y. Deuteration isotope effect on nonradiative transition of fac-tris (2-phenylpyridinato) iridium (III) complexes. *Chem. Phys. Lett.* **2010**, *491*, 199–202.
29. Tong, C.C.; Hwang, K.C. Enhancement of OLED efficiencies and high-voltage stabilities of light-emitting materials by deuteration. *J. Phys. Chem. C* **2007**, *111*, 3490–3494.
30. Browne, W.R.; Passaniti, P.; Gandolfi, M.T.; Ballardini, R.; Henry, W.; Guckian, A.; O'Boyle, N.; McGarvey, J.J.; Vos, J.G. Probing inter-ligand excited state interaction in homo and heteroleptic ruthenium(II) polypyridyl complexes using selective deuteration. *Inorg. Chim. Acta* **2007**, *360*, 1183–1190.
31. Browne, W.R.; Vos, J.G. The effect of deuteration on the emission lifetime of inorganic compounds. *Coord. Chem. Rev.* **2001**, *219–221*, 761–787.
32. Keyes, T.E.; O'Connor, C.M.; O'Dwyer, U.; Coates, C.G.; Callaghan, P.; McGarvey, J.J.; Vos, J.G. Isotope and temperature dependence of dual emission in a mononuclear ruthenium(II) polypyridyl compound. *J. Phys. Chem. A* **1999**, *103*, 8915–8920.
33. Tang, C.W.; VanSlyke, S.A. Organic electroluminescent diodes. *Appl. Phys. Lett.* **1987**, *51*, 913:1–913:3.
34. Kohn, W.; Sham, L.J. Self-consistent equations including exchange and correlation effects. *Phys. Rev.* **1965**, *140*, A1133–A1138.
35. Soler, J.M.; Artacho, E.; Dale, J.D.; Garcia, A.; Junquera, J.; Ordejon, P.; Sanchez-Portal, D. The SIESTA method for *ab initio* order-*N* materials simulation. *J. Phys.: Condens. Matter.* **2002**, *14*, 2745–2779.
36. Perdew, J.P.; Burke, K.; Ernzerhoff, M. Generalized gradient approximation made simple. *Phys. Rev. Lett.* **1996**, *77*, 3865–3868.
37. Artacho, E.; Anglada, E.; Dieguez, O.; Gale, J.D.; Garcia, A.; Junquera, J.; Martin, R.M.; Ordejon, P.; Pruneda, J.M.; Sanchez-Portal, D.; Soler, J.M. The SIESTA method: Developments and applicability. *J. Phys.: Condens. Matter.* **2008**, *20*, 064208:1–064208:6.
38. Troullier, N.; Martins, J.L. Efficient pseudopotentials for plane-wave calculations. *Phys. Rev. B* **1991**, *43*, 1993–2006.
39. Lazzeri, M.; Vittadini, A.; Selloni, A. Structure and energetics of stoichiometric TiO₂ anatase surfaces. *Phys. Rev. B* **2001**, *63*, 155409:1–155409:9.
40. Perron, H.; Domain, C.; Roques, J.; Drot, R.; Simoni, E.; Catalette, H. Optimisation of accurate rutile TiO₂ (110), (100), (101) and (001) surface models from periodic DFT calculations. *Theor. Chem. Acc.* **2007**, *117*, 565–574.
41. Xiao, D.; Martini, L.A.; Snoeberger, R.C., III; Crabtree, R.H.; Batista, V.S. Inverse design and synthesis of acac-Coumarin anchors for robust TiO₂ sensitization. *J. Am. Chem. Soc.* **2011**, *133*, 9014–9022.
42. Pastore, M.; de Angelis, F. Aggregation of organic dyes on TiO₂ in dye-sensitized solar cells models: An *ab initio* investigation. *ACS Nano* **2010**, *4*, 556–562.
43. De Angelis, F. Direct vs. indirect injection mechanisms in perylene dye-sensitized solar cells: A DFT/TDDFT investigation. *Chem. Phys. Lett.* **2010**, *493*, 323–327.

44. De Angelis, F.; Tilocca, A.; Selloni, A. Time-Dependent DFT study of $[\text{Fe}(\text{CN})_6]^{4-}$ sensitization of TiO_2 nanoparticles. *J. Am. Chem. Soc.* **2004**, *126*, 15024–15025.
45. Li, Z.; Zhang, X.; Lu, G. Electron dynamics in dye-sensitized solar cells: Effects of surface terminations and defects. *J. Phys. Chem. B* **2010**, *114*, 17077–17083.
46. Duncan, W.R.; Prezhdoo, O.V. Temperature independence of the photoinduced electron injection in dye-sensitized TiO_2 rationalized by ab initio time-domain density functional theory. *J. Am. Chem. Soc.* **2008**, *130*, 9756–9762.
47. Mosconi, E.; Yum, J.-H.; Kessler, F.; Gomez Garcia, C.J.; Zuccaccia, C.; Cinti, A.; Nazeeruddin, Md.K.; Grätzel, M.; de Angelis, F. Cobalt electrolyte/dye interactions in dye-sensitized solar cells: a combined computational and experimental study. *J. Am. Chem. Soc.* **2012**, *134*, 19438–19453.
48. Daeneke, T.; Mozer, A.J.; Uemura, Y.; Makuta, S.; Fekete, M.; Tachibana, Y.; Koumura, N.; Bach, U.; Spicca, L. Dye regeneration kinetics in dye-sensitized solar cells. *J. Am. Chem. Soc.* **2012**, *134*, 16925–16928.
49. Ahmad, S.; Bessho, T.; Kessler, F.; Baranoff, E.; Frey, J.; Yi, C.; Grätzel, M.; Nazeeruddin, Md.K. A new generation of platinum and iodine free efficient dye-sensitized solar cells. *Phys. Chem. Chem. Phys.* **2012**, *14*, 10631–10639.
50. Dos Santos, T.; Morandeira, A.; Koops, S.; Mozer, A.J.; Tsekouras, G.; Dong, Y.; Wagner, P.; Wallace, G.; Earles, J.C.; Gordon, K.C.; Officer, D.; Durrant, J.R. Injection limitations in a series of porphyrin dye-sensitized solar cells. *J. Phys. Chem. C* **2010**, *114*, 3276–3279.
51. Koops, S.E.; O'Regan, B.C.; Barnes, P.R.F.; Durrant, J.R. Parameters influencing the efficiency of electron injection in dye-sensitized solar cells. *J. Am. Chem. Soc.* **2009**, *131*, 4808–4818.
52. Haque, S.A.; Handa, S.; Peter, K.; Palomares, E.; Thelakkat, M.; Durrant, J.R. Supermolecular control of charge transfer in dye-sensitized nanocrystalline TiO_2 films: Towards a quantitative structure-function relationship. *Angew. Chem. Int. Ed.* **2005**, *44*, 5740–5744.
53. Clifford, J.N.; Palomares, E.; Nazeeruddin, Md.K.; Grätzel, M.; Nelson, J.; Li, X.; Long, N.J.; Durrant, J.R. Molecular control of recombination dynamics in dye-sensitized nanocrystalline TiO_2 films: Free energy vs. distance dependence. *J. Am. Chem. Soc.* **2004**, *126*, 5225–5233.